PERGAMON

International Journal of Heat and Mass Transfer 45 (2002) 165–172

International Journal of HEAT and MASS TRANSFER

www.elsevier.com/locate/ijhmt

Rapid vaporization of subcooled liquid in a capillary structure

T.S. Zhao *, Q. Liao

Department of Mechanical Engineering, The Hong Kong University of Science and Technology, Clear Water Bay, Kowloon, Hong Kong, Peoples Republic of China

Received 5 December 2000

Abstract

A novel process is introduced for rapid vaporization of subcooled liquid in a capillary structure. The process consists of a low-thermal-conductivity porous wick, heated from a downward-facing grooved heating block that is in intimate contact with the upper surface of the wick structure. For such a specially configured heat transfer device, measurements show that vapor can be generated rather quickly once a sufficient amount of heat was applied. The mechanisms leading to the rapid vaporization of liquid are numerically investigated. It is found that the low thermal conductivity of the capillary structure and the presence of the extremely steep temperature gradients at the fin/porous structure interface due to the rather weak natural convection, reflected by small-scale secondary flow cells below the heated fins, are responsible for the rapid vaporization of subcooled liquid.

Keywords: Porous media; Liquid vaporization; Steam generator; Natural convection

1. Introduction

There are many circumstances in which, it is desirable to produce saturated or superheated steam instantaneously. For instance, the control of the humidity in an air-conditioned space usually requires a steam supply to have fast startup and cut-off responses. Other circumstances in which it is desirable to obtain steam instantaneously include steam body and skin therapy, steam cooking, steam hair setting, steam irons, presses and wallpaper strippers and the like. An electrically energized steam generator is usually designed such that one or more electric heaters are immersed in a water container to heat up subcooled liquid to saturated or superheated vapor. One of the major drawbacks of such a design is that it takes a rather long time for subcooled water to be vaporized because the process for heating up a large volume of water in the whole container from the subcooled liquid state to the saturated state is usually slow. In order to generate steam instantaneously, in some applications the water in the container has to be maintained at the saturated state by heaters at all time. Apparently, this will cause an extra consumption of energy due to the heat losses to the ambient.

In this work, we shall introduce a simple steam generator that enables a subcooled liquid to be vaporized rapidly. This novel rapid vapor generator consists of a low-thermal-conductivity porous wick, heated from a downward-facing grooved heating block that is in intimate contact with the upper surface of the wick structure. Subcooled liquid water enters the porous wick from its bottom and is heated by the heating block. When the heaters are switched on, the temperature of the liquid in the vicinity of the heated fin tips rises rapidly and reaches the boiling point in a very short period of time, followed by rapid vaporization of the liquid. In the meantime, menisci are formed at the vapor/liquid interface to develop a capillary force to pump subcooled liquid into the wick from the feedwater container. Thus, no external pumps are needed for the supply of the liquid water. A plurality of grooves in the heating block allow the resulting vapor to instantaneously escape from the heated surface so that a high heat transfer rate from the heating

* Corresponding author. Tel.: +852-2358-8647; fax: +852-2358-1543.

E-mail address: metzhao@ust.hk (T.S. Zhao).

0017-9310/02/$ - see front matter
PII: S0017-9310(01)00126-0

Nomenclature

A_h	upper surface area of capillary structure
c	specific heat (J/kg K)
d_p	particle diameter (mm)
g	gravitational acceleration (m/s^2)
K	permeability (m^2)
k_{eff}	effective thermal conductivity (W/m K)
L	height of the capillary structure (mm)
p	pressure (N/m^2)
Q	heating power (W)
q''	imposed heat flux (W/m^2)
T	temperature (K)
u	Darcian velocity along x-axis (m/s)
v	Darcian velocity along y-axis (m/s)
W_f	width of the fins (mm)
W_g	width of the grooves (mm)
x	coordinate in horizontal direction
y	coordinate in vertical direction

Greek symbols

α_m	thermal diffusivity (m^2/s)
β	thermal expansion coefficient (1/K)
ε	porosity
μ	viscosity ($N\ s/m^2$)
ρ	density (kg/m^3)
σ	heat capacity ratio

Subscripts

b	heating block
eff	effective value
f	fluid phase
s	solid phase

block to the saturated wick can be maintained all the time. Because of this feature, the rate of the vapor generated in this device is in nearly linear relationship with the imposed heating power, implying that the device can assure a precisely controlled instantaneous supply of a predetermined quantity of vapor. Additionally, since the device is only energized at the time when vapor is needed, the conservation of energy is assured in this device.

The primary objective of the present work was to experimentally demonstrate the heat transfer characteristics of the above-described vapor generator. Our experimental data showed that steam could be generated rather quickly as the water saturated porous medium consisting of glass beads was heated by a grooved heating block at its top. The other objective of the present work was to numerically investigate this practical problem and shed light on the heat transfer mechanisms leading to the rapid vaporization in the present device.

As mentioned earlier, the rapid vaporization of the subcooled liquid is solely due to the rapid increase of the subcooled liquid temperature before the boiling point. For this reason, we are only concerned with heat transfer characteristics in a porous medium without phase change in this work. More specifically, we shall consider the problem of transient natural convection in a liquid-saturated porous medium with its upper boundary heated by a downward-facing grooved heating block. Despite a rather substantial body of publications concerning natural convection in liquid-saturated porous enclosures due to either side heating or bottom heating [1–6], it appears that the present problem of natural convection in a porous medium with a period top heating boundary has never been reported in the literature. We shall numerically show that the low thermal conductivity of the capillary structure and the presence of the extremely steep temperature gradients at the fin/porous structure interface due to the rather weak natural convection, reflected by small-scale secondary flow cells below the heated fins, are responsible for the rapid vaporization of subcooled liquid.

2. Experimental apparatus

The schematic of the experimental apparatus is shown in Fig. 1. The vertically oriented rectangular capillary structure, 60.6 mm in width, 20 mm in height, and 50.6 mm in depth, was enclosed by four vertical walls, a perforated plate at its bottom, and a heating assembly at its top. The heating assembly consisted of a grooved copper block (shown in Fig. 2), a stainless steel film (0.1 mm in thickness) serving as a heater, a mica sheet (0.06 mm in thickness) serving as an electrical insulator, and an asbestos sheet (3 mm in thickness) serving as a fixture of the film heater. This heating assembly was carefully mounted on the top of the capillary structure such that the fins of the grooved block were in intimate contact with the upper surface of the capillary structure. The heating assembly was well insulated by a layer of glass fiber wool, 25 mm in thickness, covered by a teflon plate of 20 mm in thickness.

Fig. 2 shows the two grooved heating blocks (referred to as heating block I and II throughout the paper) used in the present work, which have the same total width but different widths of fins and grooves.

In this work, deionized water was used as the working fluid, which drained from the adjacent feedwater container and entered the test section from its lower section (see Fig. 1). The porous medium used in the present study consisted of glass beads, essentially

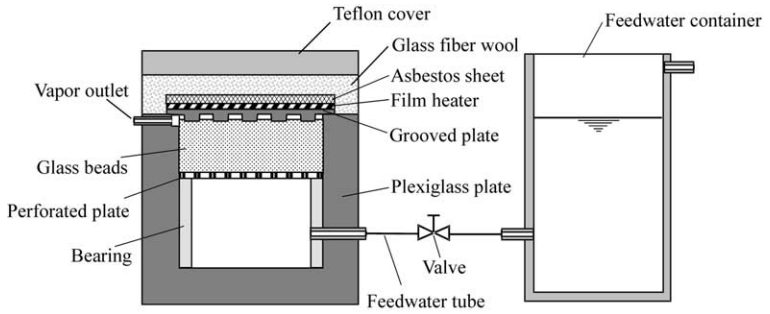

Fig. 1. Schematic of the experimental apparatus.

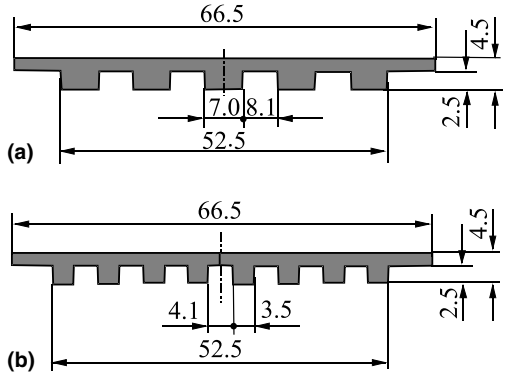

Fig. 2. Schematic of the heating blocks: (a) heating block I; (b) heating block II.

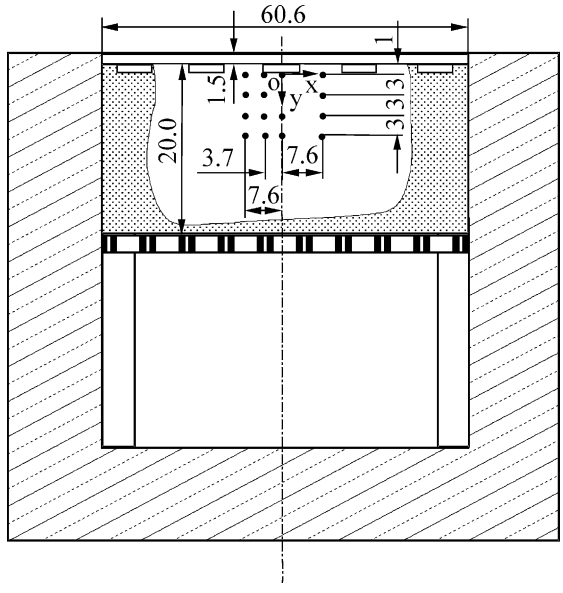

Fig. 3. Locations of the thermocouples.

spherical in shape, with an average particle diameter $d_p = 0.55$ mm. The porous medium properties such as porosity ($\varepsilon = 0.369$) and effective thermal conductivity ($k_{eff} = 0.7682$ W/m K) were measured while the permeability is determined by

$$K = \frac{\varepsilon^3 d_p^2}{180(1-\varepsilon)^2} \tag{1}$$

and the heat capacity ratio is determined by

$$\sigma = \frac{\varepsilon\rho_f c_f + (1-\varepsilon)\rho_s c_s}{\rho_f c_f}, \tag{2}$$

where the subscripts f and s denote the properties of fluid and solid media, respectively.

Temperatures were measured using fine T-type thermocouples of 0.2 mm in diameter. As shown in Fig. 3, 16 thermocouples were inserted in the porous media for measuring temperature distributions in the porous structure. Two thermocouples were installed into the grooves of the heating block to measure the temperature of the generated vapor, while the other two were used to measure the wall temperatures of the heating block. A data acquisition system, consisting of a personal computer, an A/D converter board (MetraByte DAS-20), and two universal analog input multiplexers (MetraByte EXP-20), was employed to record the temperature measurements.

Prior to each experiment, the water level of the feedwater container was adjusted to be above the top of the porous structure such that the porous structure could be degassed. After half an hour of degassing, the water level was adjusted back to the upper surface of the porous structure. For each test case, the transient temperatures in the porous structure and in the grooves of the heating block were measured. The time for vapor generation, denoted by Δt, was determined by accounting elapsed time from the instance of switching on the heating power supply to the instance at which the temperatures in the vapor grooves in the heating block reached the saturated value.

In the present study, the heat flux imposed to the capillary structure is determined by

$$q'' = \frac{(Q - Q_b)}{A_h}, \tag{3}$$

where A_h denotes the upper surface area of the capillary structure, Q is the heating power, Q_b is the heat absorbed by the grooved heating block during the water vaporization time Δt and is estimated by

$$Q_b = M_b c_b (T_{be} - T_{bi})/\Delta t, \tag{4}$$

where M_b and c_b are the mass and the specific heat of the grooved heating block, T_{bi} is the wall temperature of the heating block before applying heating power while T_{be} is the wall temperature of the heating block at the instance when steam is generated.

The heating power was measured with a multimeter having an accuracy of ±0.6% in electric voltage reading and ±0.15% in electric current reading. The thermocouples were calibrated to ensure the accuracy within ±0.2°C. The uncertainty in measuring vaporization time Δt was estimated to be less than ±2%. The heat loss was estimated to be about 8%. Using the uncertainty estimation method of Kline and McClintock [7], it was estimated that the uncertainty of the imposed heat flux q'' was within 8.5%.

3. Numerical investigation

We now numerically analyze the above-described physical problem. Because geometrically the grooves are symmetric with respect to the middle of each fin of the heating block (see Fig. 1), we only need to consider a unit cell of the porous structure shown in Fig. 4. The two-dimensional unit cell is enclosed by a upper and lower boundaries having a total width of $W_f + W_g$, one fin (W_f in width) with two half grooves (W_g in width), and two vertical symmetric walls having a height of $L = 20$ mm. To simplify the analysis, we assume that the porous medium is rigid, uniform, isotropic and fully saturated with fluid. It is further assumed that the thermophysical properties of both solid and fluid are assumed to be constant and the fluid and solid phases are in local thermal equilibrium. Darcy's law, together with the Boussinesq approximation and negligible thermal dispersion, leads to the following governing equations [1–3]:

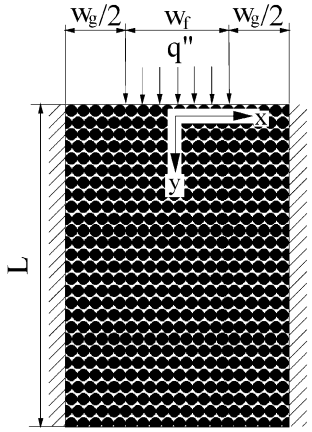

Fig. 4. Unit cell for numerical investigation.

$$\frac{\partial u}{\partial x} + \frac{\partial v}{\partial y} = 0, \tag{5}$$

$$u = -\frac{K}{\mu}\frac{\partial P}{\partial x}, \tag{6}$$

$$v = -\frac{K}{\mu}\left[\frac{\partial P}{\partial y} - \rho\beta g(T - T_c)g\right], \tag{7}$$

$$\sigma\frac{\partial T}{\partial t} + u\frac{\partial T}{\partial x} + v\frac{\partial T}{\partial y} = \alpha_m\left(\frac{\partial^2 T}{\partial x^2} + \frac{\partial^2 T}{\partial y^2}\right). \tag{8}$$

The relevant boundary conditions (see Fig. 4) are given by at $x = -(W_f + W_g)/2$ (symmetric left side wall)

$$\frac{\partial u}{\partial x} = 0, \tag{9}$$

$$\frac{\partial T}{\partial x} = 0 \tag{10}$$

at $x = (W_f + W_g)/2$ (symmetric right side wall)

$$\frac{\partial u}{\partial x} = 0, \tag{11}$$

$$\frac{\partial T}{\partial x} = 0 \tag{12}$$

at $y = 0$ (upper boundary)

$$u = 0; \quad v = 0 \quad \text{(impermeable)} \tag{13}$$

$$-k_{eff}\frac{\partial T}{\partial x} = \begin{cases} 0 & \text{if } -(W_f + W_g)/2 \leqslant x \leqslant -W_f/2, \\ q'' & \text{if } -W_f/2 \leqslant x \leqslant W_f/2, \\ 0 & \text{if } W_f/2 \leqslant x \leqslant (W_f + W_g)/2 \end{cases} \tag{14}$$

at $y = L$ (lower boundary)

$$u = 0; \quad v = 0 \quad \text{(impermeable)}, \tag{15}$$

$$T = T_c. \tag{16}$$

All the symbols used in the governing equations and the boundary conditions are defined in the Nomenclature.

A numerical solution for Eqs. (5)–(8) subjected to the boundary conditions (9)–(16) was obtained based on a control-volume method detailed by Patankar [8]. The equations were solved as a simultaneous set, and convergence was achieved with the criterion that the relative errors between iterations in both the enthalpy and velocity fields be less than 10^{-5}, and that mass and energy conservation in the system was ensured to within 0.1%. A series of test runs were performed to ensure that

the numerical results were independent of the grid size. The choice of 26×82 uniform grid points was found to provide grid independence for the results reported in this paper.

4. Results and discussion

The experiments were conducted for the same porous structure and for two heating cooper blocks having the same total width but different widths of grooves and fins (see Fig. 2). The applied heat flux was varied from 17.9 to 44.1 kW/m^2 while keeping the inlet temperature of the subcooled water at $T_c = 26$°C.

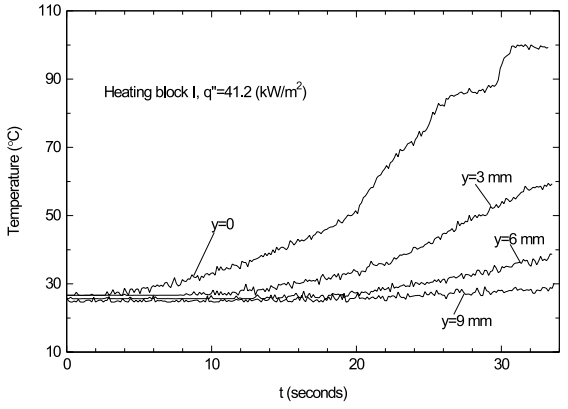

Fig. 5. Measured temperatures at different elevations in the porous structure heated by the heating block I at $q'' = 41.2$ kW/m^2.

Fig. 5 presents the time-dependent temperatures at different elevations in the porous medium ($y = 0$, 3, 6, and 9 mm) heated by the heating block I with a heat flux of $q'' = 41.2$ kW/m^2. It is shown that once the specified heat flux was applied, the temperature at the upper surface of the porous structure ($y = 0$) rose rapidly, taking only about 30 s from the subcooled water temperature of 26°C to the saturated steam temperature. Subsequently, produced steam was observed in the vapor outlet of the test setup. On the other hand, it is seen from Fig. 5 that the increase of the temperatures becomes progressively slow at the locations away from the upper surface of the porous medium, and the temperature at $y = 9$ mm remained almost the same as the feedwater temperature $T_c = 26$°C. The mechanisms leading to the rapid vaporization of subcooled liquid adjacent to the heated fin can be explained based on the numerical results presented in the followings.

Fig. 6 represents the isotherms and the velocity vectors in the unit cell of the porous structure at the instance of 30 s. As shown in Fig. 6(a), rather sharp temperature gradients occur around the heated fin, whereas the temperatures in most regions of the porous structure remain almost the same as the inlet temperature of the subcooled liquid. The velocity vectors presented in Fig. 6(b) show that two symmetric secondary flow cells exist underneath the heated fin. However, both

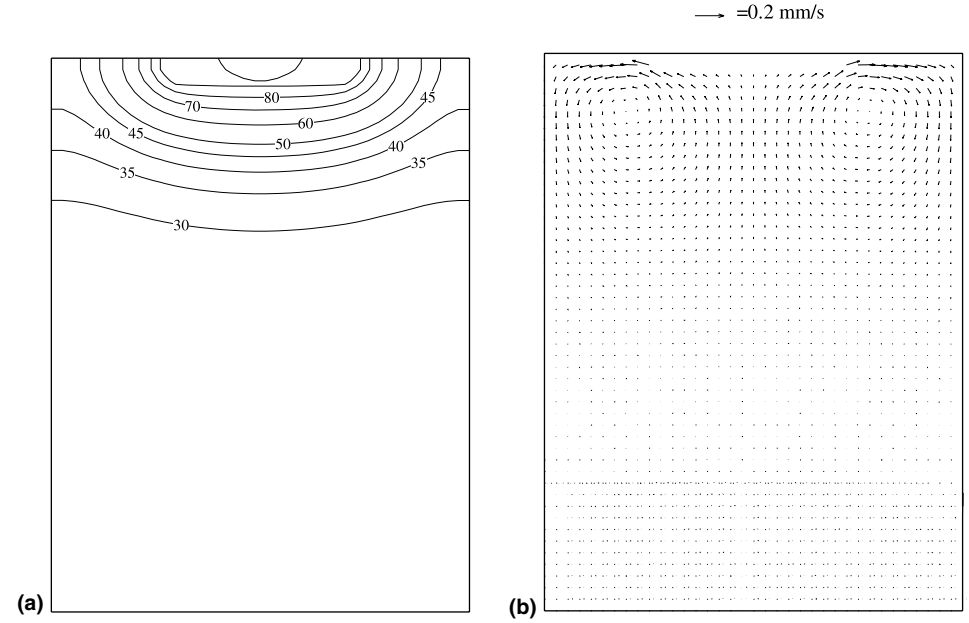

Fig. 6. Numerical results at the instance of 30 s for the case using heating block I at $q'' = 41.2$ kW/m^2 and $k_{eff} = 0.7432$ W/m K: (a) isotherms and (b) velocity vectors.

the velocity magnitudes and the scale of the flow cells are extremely small, indicating the natural convection for the present heat transfer configuration is rather weak. The weak buoyancy-induced flow in the present configured heat transfer device is primarily because the porous structure is heated from its top boundary. Furthermore, the rather small effective thermal conductivity of the glass-water system confines the secondary flow cells close to the top of the porous structure. This can be further evident from Fig. 7, where the isotherms and the velocity vectors for the case of a larger effective of thermal conductivity ($k_{\text{eff}} = 3.2$ W/m K) are presented. The isotherms shown in Fig. 7(a) indicates that for the case of the higher effective thermal conductivity, the temperature gradients around the heated fin become relatively small and the higher temperature region become substantially large as compared with the case of the lower thermal conductivity. It is also seen from the velocity vectors presented in Fig. 7(b) that the flow cells expand downwardly as compared with the case presented in Fig. 7(b) for the case of the lower thermal conductivity.

Apparently, the numerical solution presented above shows that for the present specially devised heat transfer configuration, heat transfer from the heated fin to the liquid saturated porous medium due to natural convection is rather weak. In addition, the very low effective thermal conductivity of the glass-water system results in rather small amount of heat energy conducted to the fluid in the lower portion of the porous structure. Therefore, almost all the heat energy added to the porous structure through the heating block is accumulated at the interface between the heated fin and the porous structure, thereby leading to the rapid increase of the local temperature and eventually resulting in extremely rapid vaporization of the subcooled liquid to the interface.

We now present the effect of the grooved heating blocks on the vaporization time. Both the numerically predicted values (represented by solid and dashed lines) and the experimental data (represented by solid circles and empty squares) of the vaporization time Δt for the two heating blocks I and II is shown in Fig. 8. It is seen that the numerical results are in fair agreement with the experimental data. Apparently, the vaporization time Δt was decreased progressively with the increase of the heat flux. The comparison between the two heating blocks I and II indicates that the wider fins (Block II) resulted more rapid vaporization of subcooled liquid. This is because the wider heated fins impeded the development of the secondary flow cells in the porous medium, thereby the natural convection becoming weaker.

Fig. 9 presents the variation of the temperatures along the middle line of the porous structure heated using the two heating blocks I and II at the instance of 30 s. Both numerical and experimental results are displayed. Once again, the numerical solution is in reasonable agreement with the experimental data. The variation of temperatures remains relatively flat in the lower portion of the porous structure and becomes extremely steep adjacent to the top of the porous structure.

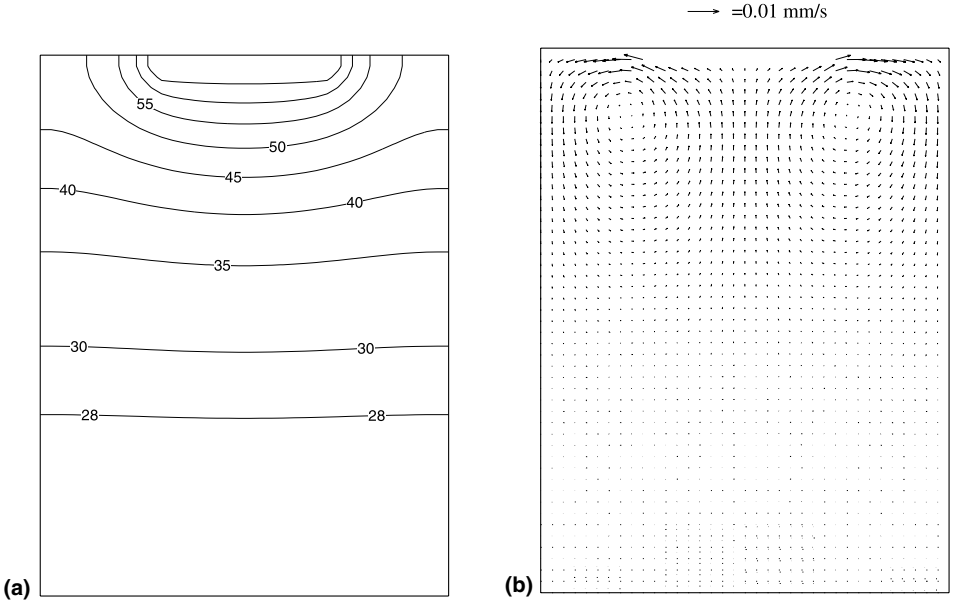

Fig. 7. Numerical results at the instance of 30 s for the case using heating block I at $q'' = 41.2$ kW/m^2 and $k_{\text{eff}} = 3.2$ W/m K: (a) isotherms and (b) velocity vectors.

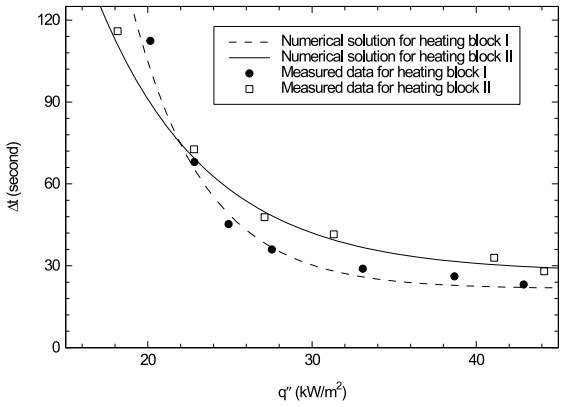

Fig. 8. Vaporization time at different heat fluxes for two heating blocks.

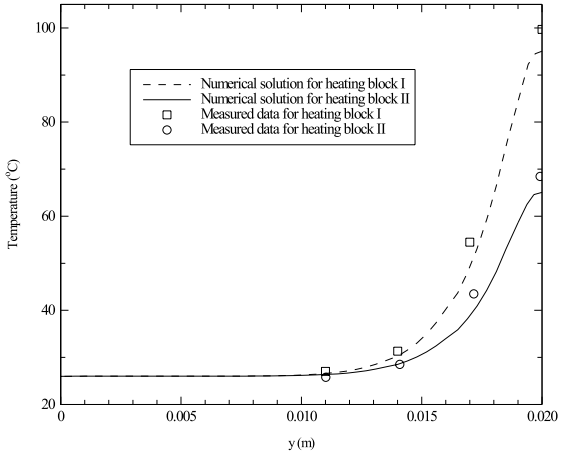

Fig. 9. Temperature distribution along the y-axis for two heating blocks at $q'' = 41.2$ kW/m^2.

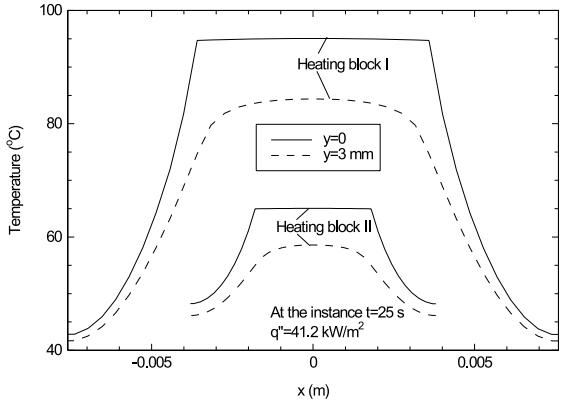

Fig. 10. Temperature distribution along the x-axis for two heating blocks at $q'' = 41.2$ kW/m^2.

In particular, the block II with wider fins resulted in steeper temperature gradients close to the top of the porous structure. Hence, for the same heat flux, the block II will lead to a higher temperature at the interface between the heated fin and the porous structure. The temperature variations along the x-axis at the top and a distance of 3 mm from the top of the porous structure are displayed in Fig. 10. For each heating block, the temperatures beneath the fin are seen much higher than beneath the groove. It can also be evident from Fig. 10 that using the heating block I leads to a higher temperature at the top of the porous structure.

5. Concluding remarks

In this work, we have shown that as a liquid saturated, low-thermal-conductivity porous structure is heated using a grooved heating block placed at its top, vapor can be produced rather quickly. The numerical solution indicates that the presence of the extremely steep temperature gradients at the fin/porous structure interface due to the rather weak natural convection, reflected by small-scale secondary flow cells below the heated fins, and the low thermal conductivity of the porous structure are responsible for the rapid vaporization of liquid. This unique feature can be used to devise a rapid vapor generator, which may have a wider variety of applications such as humidity control, steam cooking, steam hair setting, steam skin therapy, steam irons, and the like.

Acknowledgements

This work was supported by Hong Kong RGC Earmarked Research Grants No. HKUST 6178/00E. The first author gratefully acknowledges the Visiting Scholar Foundation of the State Key Laboratory of Multiphase Flow in Power Engineering at Xi'an Jiaotong University.

References

[1] P. Cheng, Heat transfer in geothermal systems, Advances in Heat Transfer, vol. 14, Academic Press, New York, 1978, pp. 1–105.
[2] D.A. Nield, A. Bejan, Convection in Porous Media, Springer, New York, 1992.
[3] M. Kaviany, Principles of Heat Transfer in Porous Media, Springer, New York, 1991.
[4] M.A. Combarnous, S.A. Bories, Hydrothermal convection in saturated porous media, Adv. Hydrosci. 10 (1975) 231–307.

[5] V. Prasad, F.A. Kulacki, M. Keyhani, Natural convection in porous media, J. Fluid Mech. 150 (1985) 89–119.
[6] D.C. Reda, Natural convection experiments in a liquid-saturated porous medium bounded by vertical coaxial cylinders, J. Heat Transfer 105 (1983) 795–802.
[7] S.J. Kline, F.A. McClintock, Describing uncertainties in single-sample experiments, Mech. Eng., January 3–12, 1953.
[8] S.V. Patankar, Numerical Heat Transfer and Fluid Flow, Hemisphere, Washington, DC, 1980.